Supplementary Information

A domino effect in antifolate drug action in *Escherichia coli*

Yun Kyung Kwon[1], Wenyun Lu[1], Eugene Melamud[1], Nurussaba Khanam[2], Andrew Bognar[2], and Joshua D. Rabinowitz[1]

1 Department of Chemistry and Lewis-Sigler Institute for Integrative Genomics, Princeton University, Princeton, New Jersey 08544, United States of America

2 Department of Microbiology, University of Toronto, Toronto, Ontario, Canada M5S 1A8

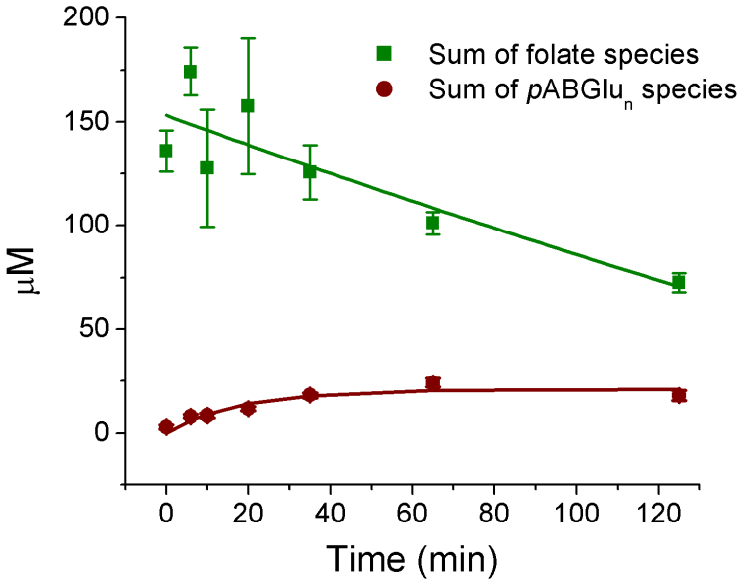

Supplementary Figure 1. Folates are slowly catabolized in response to trimethoprim treatment. Data are sums of concentrations from **Figure 1** of the main text. *p*ABGlu$_n$ is a major folate catabolite. See **Figure 1** legend for details. Error bars show ± 1 SE of the mean (n = 3 independent experiments).

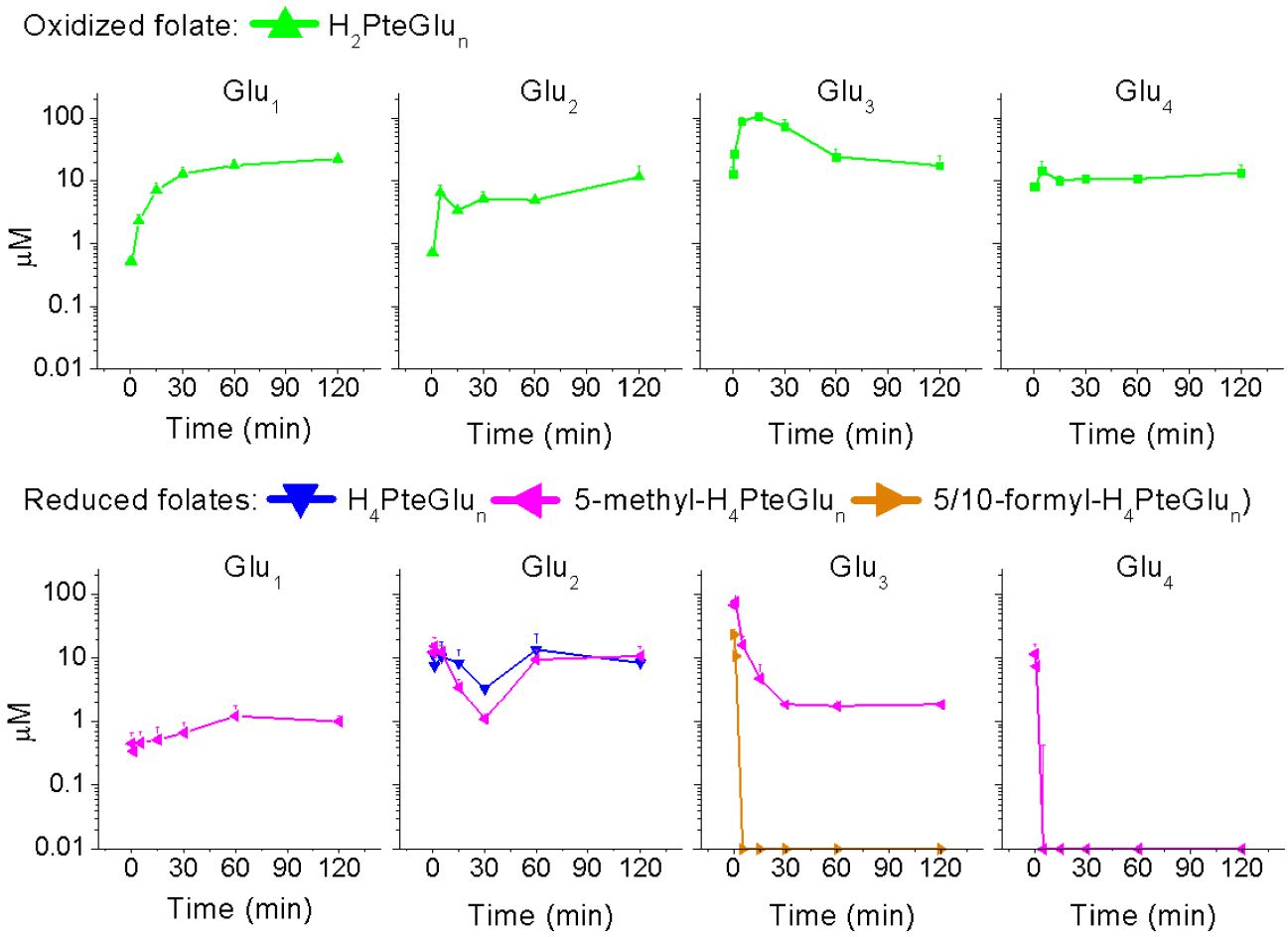

Supplementary Figure 2. A filter-culture approach that enables fast quenching of metabolism confirms that the dynamics of folates post trimethoprim treatment are not artifacts of the cell handling procedures (i.e., centrifugation). Cells were grown to A_{650} of ~ 0.5 (measured as the A_{650} after rinsing cells into 5 ml of water) on nylon filters resting on media-loaded agarose plates and then switched to media-loaded agarose plates containing 4 µg ml^{-1} trimethoprim. The density of cells on the filter was such that most cells are in direct contact with the filter and thus nutrient source and drug. Metabolism was quenched by direct and immediate transfer of the filters into –75°C extraction solvent, and extraction was carried out as described in *Methods*. The *x* axis represents minutes after drug addition, the *y* axis represents peak intensities on a log scale, and the error bars show + 1 SE of the mean (n = 3 independent experiments). Fewer folate species are detected when cells are grown on filters on plates because fewer cells are harvested (8-fold less than 40 ml of liquid culture of comparable A_{650}) and a higher extraction volume is required (2.5 ml versus 400 µl).

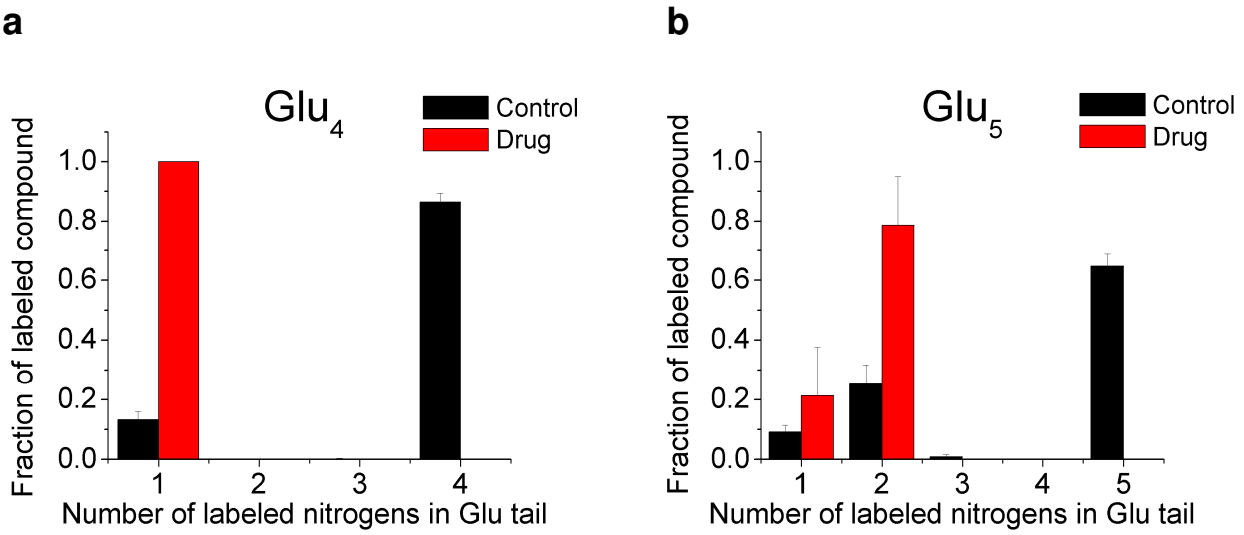

Supplementary Figure 3. ^{15}N-assimilation patterns into folates reveal that folylpoly-α-glutamate synthetase (FP-α-GS) activity is not affected by trimethoprim treatment. In control cells, the majority of folate species contain fully ^{15}N-labeled glutamate tails 2 hours post N-isotope switch. In drug treated cells, folate-Glu_4 species contain only one ^{15}N-label in their glutamate tails while -Glu_5 species contain one or two ^{15}N-labels in their glutamate tails. The ^{15}N-labels likely occur in the last glutamate residue in $H_2PteGlu_4$ and the last two glutamate residues in $H_2PteGlu_5$. The 4th and 5th glutamate residues are added by FP-α-GS (not FP-γ-GS) and are bonded via α-linkages to previous glutamates. 5-methyl-$H_4PteGlu_{4,5}$ data are shown for control cells, and $H_2PteGlu_{4,5}$ are shown for drug-treated cells, as they are the most abundant folate species with 4 and 5 glutamate residues in their tails in control and trimethoprim-treated cells, respectively. Error bars show + 1 SE of the mean (n = 3 independent experiments).

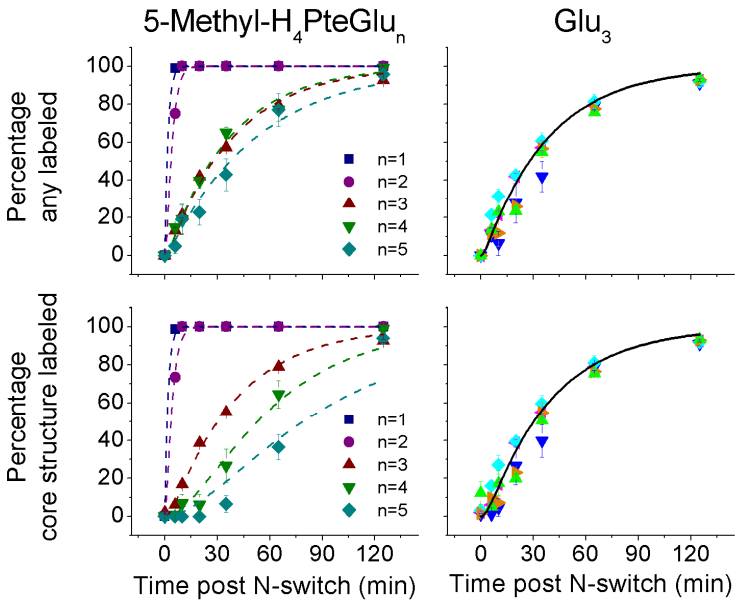

Supplementary Figure 4. Probing folate fluxes in control cells by monitoring ^{15}N-assimilation. Control *E. coli* cells were grown to log phase in ^{14}N-media and then switched to ^{15}N-media. (**Left**) Incorporation of ^{15}N into 5-methyl-H_4PteGlu$_n$, n = 1-5. Folate mono- and diglutamate species (which are present in cells in low concentrations) quickly become labeled. In contrast, labeling of the folates with longer glutamate tails (which are present in cells in higher concentrations) occurs more slowly, with passage of core labeling to the longest glutamate chain species most delayed. This pattern of labeling is consistent with the known enzyme mechanism involving extension of the glutamate chain one residue at a time. (**Right**) Different oxidation and one-carbon states of a given glutamate chain length (**H_2PteGlu$_3$, H_4PteGlu$_3$, 5,10-methylene-H_4PteGlu$_3$, 5-methyl-H_4PteGlu$_3$,** and **5/10-formyl-H_4PteGlu$_3$**) all show indistinguishable labeling kinetics. This is consistent with each glutamate-addition step being slow relative to the oxidation-reduction and one-carbon transfer reactions in which folates also participate (if an oxidation-reduction or one-carbon transfer reaction were slow, labeling of the product species would be measurably delayed). The *x* axis represents minutes post N-switch. In the top row, the *y* axis represents the percent of folates containing ≥ one ^{15}N atom (any labeled). In the bottom row, the *y* axis represents the percent of folates containing ≥ one ^{15}N atom in the pteroate portion of the molecule (core structure labeled). Error bars show ± 1 SE of the mean (n = 3 independent experiments). Curves represent a fit of the data as per Yuan et. al[1], as described in *Methods*.

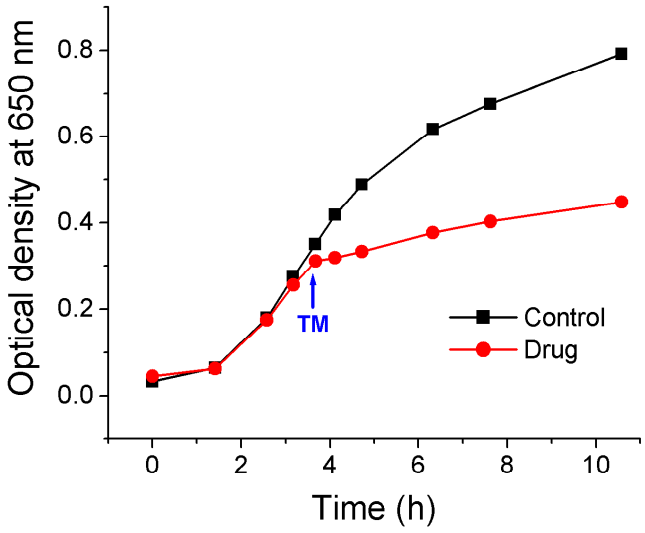

Supplementary Figure 5. Effect of trimethoprim on growth of *E. coli* in a shaking flask at 37°C in a minimal salts media[2] with 10 mM ammonium chloride as the nitrogen source and 0.4% glucose as the carbon source. 4 μg ml^{-1} trimethoprim was added at the time indicated by the arrow.

Supplementary Table 1. LC-MS/MS parameters for compounds of interest. The LC approach was hydrophilic interaction chromatography (HILIC) with an amino column, and MS/MS detection was by scanning through numerous multiple reaction monitoring (MRM) events on a triple quadrupole instrument. Samples were stored (4°C) for a maximum of 12 h prior to analysis to minimize folate degradation. All analyses were performed on a Finnigan TSQ Quantum Ultra triple quadrupole mass spectrometer (Thermo Electron Corporation, San Jose, CA) equipped with electrospray ionization (ESI) source, coupled to a LC-10A HPLC system (Shimadzu, Columbia, MD).

Compound	Parent formula	Number of ^{15}N in parent	Parent *m/z**	Collision energy (eV)	Product formula	Number of ^{15}N in product	Product *m/z**	RT (min)
Trimethoprim	$C_{14}H_{19}N_4O_3^+$		291.100	23	$C_5N_4H_7^+$		123	2.3
GMP	$C_{10}H_{15}N_5O_8P^+$	0	364.06	19	$C_5H_6N_5O^+$	0	152	5.8
		1	365.06	19		1	153	
		2	366.06	19		2	154	
		3	367.06	19		3	155	
		4	368.05	19		4	156	
		5	369.05	19		5	157	
GTP	$C_{10}H_{17}N_5O_{14}P_3^+$	0	524	37	$C_5H_6N_5O^+$	0	152	7.1
		1	525	37		1	153	
		2	526	37		2	154	
		3	527	37		3	155	
		4	528	37		4	156	
		5	529	37		5	157	
*p*ABGlu$_1$	$C_{12}H_{15}N_2O_5^+$	0	267.1	18	$C_7H_6NO^+$	0	120.04	6.1
		1	268.1	18		0	120.05	
		1	268.11	18		1	121.04	
		2	269.1	18		1	121.05	
*p*ABGlu$_2$	$C_{17}H_{22}N_3O_8^+$	0	396.14	25	$C_7H_6NO^+$	0	120.04	6.2
		1	397.13	25		0	120.05	
		1	397.14	25		1	121.04	
		2	398.13	25		0	120.05	
		2	398.14	25		1	121.03	
		3	399.13	25		1	121.06	

Compound	Parent formula	Number of ^{15}N in parent	Parent *m/z**	Collision energy (eV)	Product formula	Number of ^{15}N in product	Product *m/z**	RT (min)
*p*ABGlu$_3$	$C_{22}H_{29}N_4O_{11}^+$	0	525.18	35	$C_7H_6NO^+$	0	120.04	6.3
		1	526.18	35		0	120.05	
		1	526.19	35		1	121.05	
		2	527.18	35		0	120.03	
		2	527.19	35		1	121.03	
		3	528.17	35		0	120.06	
		3	528.18	35		1	121.06	
		4	529.17	35		1	121.04	
*p*ABGlu$_4$	$C_{27}H_{36}N_5O_{14}^+$	0	654.22	43	$C_7H_6NO^+$	0	120.05	6.8
		1	655.22	43		0	120.04	
		1	655.23	43		1	121.05	
		2	656.22	43		0	120.05	
		2	656.24	43		1	121.04	
		3	657.22	43		0	120.05	
		3	657.23	43		1	121.04	
		4	658.21	43		0	120.03	
		4	658.22	43		1	121.04	
		5	659.21	43		1	121.06	
PteGlu$_1$	$C_{19}H_{20}N_7O_6^+$	0	442.15	27	$C_{14}H_{11}N_6O_2^+$	0	295.08	6.6
PteGlu$_2$	$C_{24}H_{27}N_8O_9^+$	0	571.19	30	$C_{14}H_{11}N_6O_2^+$	0	295.1	6.8
PteGlu$_3$	$C_{29}H_{34}N_9O_{12}^+$	0	700.230	32	$C_{14}H_{11}N_6O_2^+$	0	295.09	7
		1	701.230	32		0	295.1	
		1	701.240	32		1	296.1	
		2	702.220	32		0	295.11	
		2	702.230	32		1	296.11	
		3	703.210	32		0	295.08	
		3	703.220	32		1	296.08	
		4	704.220	32		1	296.1	
		5	705.220	32		2	297.1	
		6	706.210	32		3	298.09	
		7	707.210	32		4	299.08	
		8	708.210	32		5	300.08	
		9	709.210	32		6	301.08	

Compound	Parent formula	Number of 15N in parent	Parent m/z*	Collision energy (eV)	Product formula	Number of 15N in product	Product m/z*	RT (min)
$PteGlu_4$	$C_{34}H_{41}N_{10}O_{15}^+$	0	829.280	34	$C_{14}H_{11}N_6O_2^+$	0	295.09	7.3
		1	830.270	34		0	295.1	
		1	830.280	34		1	296.1	
		2	831.280	34		0	295.1	
		3	832.280	34		0	295.1	
		4	833.280	34		0	295.1	
		5	834.280	34		1	296.1	
		6	835.270	34		2	297.1	
		7	836.270	34		3	298.1	
		8	837.270	34		4	299.1	
		9	838.260	34		5	300.1	
		10	839.260	34		6	301.1	
$PteGlu_5$	$C_{39}H_{48}N_{11}O_{18}^+$	0	958.32	42	$C_{14}H_{11}N_6O_2^+$	0	295.09	8
		1	959.32	42		0	295.09	
		2	960.32	42		0	295.09	
		3	961.32	42		0	295.09	
		4	962.32	42		0	295.09	
		5	963.32	42		0	295.09	
		6	964.31	42		1	296.09	
		7	965.31	42		2	297.09	
		8	966.31	42		3	298.09	
		9	967.31	42		4	299.09	
		10	968.3	42		5	300.09	
		11	969.3	42		6	301.09	
$H_2PteGlu_1$	$C_{19}H_{22}N_7O_6^+$	0	444.16	27	$C_7H_8O_5N^+$	0	178.07	6.1
		1	445.16	27		0	178.07	
		2	446.16	27		0	178.07	
		3	447.15	27		1	179.07	
		4	448.15	27		2	180.07	
		5	449.15	27		3	181.06	
		6	450.15	27		4	182.06	
		7	451.14	27		5	183.06	

Compound	Parent formula	Number of 15N in parent	Parent m/z*	Collision energy (eV)	Product formula	Number of 15N in product	Product m/z*	RT (min)
$H_2PteGlu_2$	$C_{24}H_{29}N_8O_9^+$	0	573.21	30	$C_7H_8O_5N^+$	0	178.07	
		1	574.2	30		0	178.06	
		2	575.2	30		0	178.05	
		3	576.2	30		0	178.04	
		4	577.2	30		1	179.07	
		5	578.19	30		2	180.07	
		6	579.19	30		3	181.07	
		7	580.19	30		4	182.07	
		8	581.18	30		5	183.07	
$H_2PteGlu_3$	$C_{29}H_{36}N_9O_{12}^+$	0	702.250	35	$C_7H_8O_5N^+$	0	178.07	6.7
		1	703.240	35		0	178.06	
		1	703.250	35		1	179.06	
		2	704.230	35		0	178.08	
		3	705.240	35		0	178.06	
		4	706.240	35		0	178.07	
		5	707.230	35		1	179.06	
		6	708.230	35		2	180.07	
		7	709.230	35		3	181.06	
		8	710.220	35		4	182.05	
		9	711.230	35		5	183.06	
$H_2PteGlu_4$	$C_{34}H_{43}N_{10}O_{15}^+$	0	831.29	40	$C_7H_8O_5N^+$	0	178	7.1
		1	832.27	40		1	179	
		1	832.28	40		0	178	
		2	833.28	40		0	178	
		3	834.28	40		0	178	
		4	835.27	40		0	178	
		5	836.27	40		0	178	
		6	837.27	40		1	179	
		7	838.26	40		2	180	
		8	839.26	40		3	181	
		9	840.26	40		4	182	
		10	841.25	40		5	183	

Compound	Parent formula	Number of 15N in parent	Parent m/z*	Collision energy (eV)	Product formula	Number of 15N in product	Product m/z*	RT (min)
$H_2PteGlu_5$	$C_{39}H_{50}N_{11}O_{18}^+$	0	960.33	42	$C_7H_8O_5N^+$	0	178.07	8
		1	961.33	42		0	178.07	
		2	962.33	42		0	178.07	
		3	963.33	42		0	178.07	
		4	964.32	42		0	178.07	
		5	965.32	42		0	178.07	
		6	966.32	42		0	178.07	
		7	967.31	42		1	179.07	
		8	968.31	42		2	180.07	
		9	969.31	42		3	181.07	
		10	970.31	42		4	182.07	
		11	971.31	42		5	183.07	
$H_4PteGlu_1$	$C_{19}H_{24}N_7O_6^+$	0	446.18	20	$C_{14}H_{15}N_6O_2^+$	0	299.13	6.2
		1	447.17	20		1	300.12	
		1	447.18	20		0	299.12	
		2	448.16	20		2	301.13	
		2	448.17	20		1	300.12	
		3	449.16	20		3	302.12	
		3	449.17	20		2	301.12	
		4	450.16	20		4	303.13	
		4	450.17	20		3	302.13	
		5	451.16	20		5	304.12	
		5	451.17	20		4	303.12	
		6	452.16	20		6	305.13	
		6	452.17	20		5	304.13	
$H_4PteGlu_2$	$C_{24}H_{31}N_8O_9^+$	0	575.22	30	$C_{14}H_{15}N_6O_2^+$	0	299.12	6.4
		1	576.22	30		0	299.13	
		2	577.21	30		0	299.14	
		2	577.22	30		1	300.13	
		3	578.21	30		1	300.13	
		4	579.21	30		2	301.14	
		5	580.2	30		3	302.14	
		6	581.2	30		4	303.14	
		7	582.2	30		5	304.13	
		8	583.2	30		6	305.12	

Compound	Parent formula	Number of 15N in parent	Parent m/z*	Collision energy (eV)	Product formula	Number of 15N in product	Product m/z*	RT (min)
$H_4PteGlu_3$	$C_{29}H_{38}N_9O_{12}^+$	0	704.26	35	$C_{14}H_{15}N_6O_2^+$	0	299.13	6.7
		1	705.26	35		0	299.14	
		1	705.27	35		1	300.12	
		2	706.25	35		0	299.12	
		2	706.26	35		1	300.13	
		3	707.25	35		0	299.13	
		3	707.26	35		1	300.13	
		4	708.24	35		1	300.12	
		4	708.25	35		2	301.14	
		5	709.24	35		2	301.13	
		5	709.25	35		3	302.14	
		6	710.24	35		3	302.14	
		6	710.25	35		4	303.13	
		7	711.23	35		4	303.14	
		7	711.24	35		5	304.13	
		8	712.24	35		5	304.11	
		8	712.25	35		6	305.11	
		9	713.24	35		5	304.12	
		9	713.25	35		6	305.12	
5,10-methylene-$H_4PteGlu_3$	$C_{30}H_{38}N_9O_{12}^+$	0	716.26	35	$C_{15}H_{15}N_6O_2^+$	0	311.13	6.8
		1	717.26	35		0	311.12	
		1	717.27	35		1	312.12	
		2	718.25	35		0	311.12	
		2	718.26	35		1	312.13	
		3	719.25	35		1	312.12	
		3	719.26	35		0	311.13	
		4	720.25	35		1	312.13	
		5	721.25	35		2	313.13	
		6	722.25	35		3	314.13	
		7	723.25	35		4	315.13	
		8	724.24	35		5	316.13	
		9	725.24	35		6	317.13	

Compound	Parent formula	Number of 15N in parent	Parent m/z*	Collision energy (eV)	Product formula	Number of 15N in product	Product m/z*	RT (min)
5,10-methylene-H_4PteGlu$_4$	$C_{35}H_{45}N_{10}O_{15}^+$	0	845.31	40	$C_{15}H_{15}N_6O_2^+$	0	311.13	7.2
		1	846.3	40		0	311.14	
		1	846.31	40		1	312.12	
		2	847.29	40		0	311.14	
		2	847.3	40		1	312.13	
		3	848.29	40		0	311.15	
		3	848.3	40		1	312.15	
		4	849.29	40		0	311.13	
		4	849.3	40		1	312.13	
		5	850.29	40		1	312.12	
		6	851.29	40		2	313.12	
		7	852.29	40		3	314.13	
		8	853.28	40		4	315.13	
		9	854.28	40		5	316.13	
		9	854.29	40		6	317.13	
		10	855.28	40		6	317.12	
5-methyl-H_4PteGlu$_1$	$C_{20}H_{26}N_7O_6^+$	0	460.19	25	$C_{15}H_{17}N_6O_2^+$	0	313.14	6.2
		1	461.19	25		0	313.13	
		1	461.2	25		1	314.13	
		2	462.19	25		1	314.14	
		2	462.2	25		2	315.14	
		3	463.19	25		2	315.12	
		3	463.2	25		3	316.12	
		4	464.18	25		3	316.13	
		4	464.19	25		4	317.13	
		5	465.18	25		4	317.12	
		5	465.19	25		5	318.12	
		6	466.18	25		5	318.13	
		6	466.19	25		6	319.13	
		7	467.17	25		6	319.12	

Compound	Parent formula	Number of 15N in parent	Parent m/z*	Collision energy (eV)	Product formula	Number of 15N in product	Product m/z*	RT (min)
5-methyl-H_4PteGlu$_2$	$C_{25}H_{33}N_8O_9^+$	0	589.24	28	$C_{15}H_{17}N_6O_2^+$	0	313.14	6.3
		1	590.23	28		0	313.13	
		1	590.24	28		1	314.13	
		2	591.22	28		0	313.12	
		2	591.23	28		1	314.12	
		3	592.22	28		1	314.13	
		3	592.23	28		2	315.13	
		4	593.22	28		2	315.12	
		4	593.23	28		3	316.12	
		5	594.21	28		3	316.13	
		5	594.22	28		4	317.13	
		6	595.21	28		4	317.12	
		6	595.22	28		5	318.12	
		7	596.22	28		5	318.14	
		7	596.23	28		6	319.14	
		8	597.21	28		6	319.12	
5-methyl-H_4PteGlu$_3$	$C_{30}H_{40}N_9O_{12}^+$	0	718.28	32	$C_{15}H_{17}N_6O_2^+$	0	313.14	6.7
		1	719.28	32		0	313.13	
		1	719.29	32		1	314.14	
		2	720.26	32		0	313.14	
		2	720.27	32		1	314.13	
		3	721.25	32		0	313.13	
		3	721.26	32		1	314.15	
		4	722.25	32		1	314.13	
		4	722.26	32		2	315.13	
		5	723.24	32		2	315.13	
		5	723.25	32		3	316.14	
		6	724.24	32		3	316.13	
		6	724.25	32		4	317.14	
		7	725.25	32		4	317.13	
		7	725.26	32		5	318.13	
		8	726.26	32		5	318.14	
		8	726.27	32		6	319.12	
		9	727.26	32		6	319.12	

Compound	Parent formula	Number of 15N in parent	Parent m/z*	Collision energy (eV)	Product formula	Number of 15N in product	Product m/z*	RT (min)
5-methyl-H_4PteGlu$_4$	$C_{35}H_{47}N_{10}O_{15}^+$	0	847.32	38	$C_{15}H_{17}N_6O_2^+$	0	313.14	7.1
		1	848.32	38		0	313.13	
		1	848.33	38		1	314.14	
		2	849.31	38		0	313.13	
		2	849.32	38		1	314.13	
		3	850.3	38		0	313.12	
		3	850.31	38		1	314.12	
		4	851.29	38		0	313.11	
		4	851.3	38		1	314.11	
		5	852.29	38		1	314.13	
		6	853.28	38		2	315.12	
		7	854.29	38		3	316.11	
		8	855.29	38		4	317.13	
		9	856.3	38		5	318.12	
		9	856.31	38		6	319.12	
		10	857.3	38		6	319.11	
5-methyl-H_4PteGlu$_5$	$C_{40}H_{54}N_{11}O_{18}^+$	0	976.360	43	$C_{15}H_{17}N_6O_2^+$	0	313.14	7.6
		1	977.360	43		0	313.13	
		2	978.360	43		0	313.15	
		3	979.360	43		0	313.12	
		4	980.350	43		0	313.14	
		5	981.350	43		0	313.12	
		6	982.350	43		1	314.14	
		7	983.340	43		2	315.14	
		8	984.340	43		3	316.13	
		9	985.340	43		4	317.13	
		10	986.340	43		5	318.13	
		11	987.330	43		6	319.12	
5-formyl-H_4PteGlu$_1$	$C_{20}H_{24}N_7O_7^+$	0	474.17	20	$C_{15}H_{15}N_6O_3^+$	0	327.12	6.1
		7	481.15	20		6	333.1	

Compound	Parent formula	Number of 15N in parent	Parent m/z*	Collision energy (eV)	Product formula	Number of 15N in product	Product m/z*	RT (min)
5-formyl-H_4PteGlu$_3$	$C_{30}H_{38}N_9O_{13}^+$	0	732.260	36	$C_{15}H_{15}N_6O_3^+$	0	327.12	6.6
		1	733.260	36		0	327.13	
		1	733.270	36		1	328.13	
		2	734.240	36		0	327.14	
		2	734.250	36		1	328.12	
		3	735.240	36		0	327.11	
		3	735.250	36		1	328.11	
		4	736.240	36		1	328.13	
		5	737.230	36		2	329.12	
		6	738.230	36		3	330.11	
		7	739.230	36		4	331.1	
		8	740.140	36		5	332.11	
		8	740.150	36		6	333.11	
		9	741.230	36		5	332.13	
		9	741.240	36		6	333.13	
5-formyl-H_4PteGlu$_4$	$C_{35}H_{45}N_{10}O_{16}^+$	0	861.3	45	$C_{15}H_{15}N_6O_3^+$	0	327.12	7.1
		10	871.27	45		6	333.1	

*Decimal points were used to create a unique MRM for each isotope-labeled form of the compound of interest for record-keeping purposes and do not reflect exact masses of the compounds.

SUPPLEMENTARY METHODS

Cell handling and extraction. *E.coli* was grown in liquid culture in a shaking flask. To obtain exponential-phase cultures, saturated overnight cultures were diluted 1:30 and then grown until optical density at 650 nm (A_{650}) reached ~0.5. Cells were harvested by centrifugation of 40 ml of liquid culture for 4 min at 5000 g at room temperature. After aspiration of the supernatant, 240 µL at cold (–75°C) extraction solvent was immediately added and the sample vortexed and left to sit for 15 min at –75°C. The sample was then spun in a microcentrifuge at maximal speed for 5 min at 4°C and the supernatant taken as the first extract. The pellet was then resuspended in 160 µL of the extraction solvent and sonicated in an ice (4°C) bath for 10 min using a FS30H Ultrasonic Cleaner (Fisher Scientific) with a power of 100 W at 42 kHz. The sample was again microcentrifuged and the supernatant taken as the second extract, which was combined with the first extract to give a total of 400 µL extract. For flux profiling experiments, cell handling was as above, except with both the culture and extraction volumes reduced by 60%

For experiments involving trimethoprim, when *E. coli* cultures reached absorbance of ~0.5 at 650 nm (A_{650} of ~0.5), cells were extracted as the 0 min (control) sample. Trimethoprim (final concentration of 4 µg ml^{-1}, which is bacteriostatic in minimal media; **Supplementary Fig. 5**) was added to the remaining cell culture, and samples were extracted at the following times after drug addition (stated times include the 5 min required for centrifugation prior to quenching metabolism): 6, 10, 20, 35, 65, 125 min. To ensure centrifugation was not affecting cell metabolism, cells were also grown on filters on top of media-loaded agarose plates and directly quenched and extracted as previously described[1,3]. For details, see **Supplementary Fig. 2** legend.

Estimation of absolute folate concentrations by LC-MS/MS. Standards for the full spectrum of folates with varying glutamate chain lengths are not commercially available. Standards of 5-methyl-$H_4PteGlu_n$ (n = 1-5) are commercially available, and these species are the most abundant species in exponentially growing *E. coli* cells. Thus, 5-methyl-$H_4PteGlu_n$ (n = 1-5) standard data was used. Raw LC-MS/MS signals in units of ion counts were converted to intracellular concentrations in units of μM based on the ion count signals of known concentrations of 5-methyl-$H_4PteGlu_n$ (n = 1-5) standards spiked into extraction solution and used to extract uniformly ^{13}C-labeled *E. coli*. Raw ion counts for DHF ($H_2PteGlu_n$) and THF ($H_4PteGlu_n$) species were multiplied by a factor of 3 because the LC-MS/MS signal of $H_2PteGlu_1$ and $H_4PteGlu_1$ standards were 3-fold less than that of 5-methyl-$H_4PteGlu_1$ standards. To calculate intracellular folate concentrations in units of μM, the following conversion was used for each folate species:

$$X_n\ \mu\text{M} = \left(\frac{X_n \text{ ion counts}}{40 \text{ mL cell culture}}\right)\cdot\left(\frac{400\ \mu\text{L sample volume}}{20\ \mu\text{L injection volume}}\right) \cdot\left(\frac{20\ \mu\text{L 5-methyl-H}_4\text{PteGlu}_n \text{ standard injection volume}}{\text{5-methyl-H}_4\text{PteGlu}_n \text{ standard ion counts}}\right)\cdot\left(\frac{1\ \mu\text{g 5-methyl-H}_4\text{PteGlu}_n \text{ standard}}{1\ \text{mL}}\right) \cdot\left(\frac{50 \text{ mL cell culture}}{13.7 \text{ mg cell dry weight}}\right)\cdot\left(\frac{1000 \text{ mg cell dry weight}}{2.3 \text{ mL intracellular cell volume}}\right)\cdot\left(\frac{1}{X_n \text{ molecular weight}}\right) \quad (4)$$

where X_n is a folate species with *n* number of glutamates in its tail.

Analytical differentiation of related folate species. In the absence of ^{15}N-labeling, all folate species, except 5- versus 10-formyl-THF isomers, were differentiated by parent ion mass. LC retention time (RT) and product ion mass provided additional confirmation of folate species identity. Standard was available only for 5-formyl-THF (but not its 10-formyl isomer), and thus it was not feasible to determine whether these species could be differentiated by RT or

fragmentation. Accordingly, the associated LC-MS/MS signal is reported as 5/10-formyl-THF in **Figure 1**.

For ^{15}N-labeled forms, there is potential overlap in the parent ion masses of $PteGlu_n$, $H_2PteGlu_n$, and $H_4PteGlu_n$ species (e.g., 4-labeled $PteGlu_n$ has the same parent mass as 2-labeled $H_2PteGlu_n$ and unlabeled $H_4PteGlu_n$). The same applies to 5,10-methylene-$H_4PteGlu_n$ and 5-methyl-$H_4PteGlu_n$, which is 2 amu heavier. These potential overlaps were largely resolved by fragmentation. For example, for $PteGlu_n$ to mimic $H_2PteGlu_n$, it would not only need to have 2 ^{15}N, but also for both ^{15}N to be in the 2-amino-4-oxo-6-methylpterin portion (protonated pterin is the product ion of $H_2PteGlu_n$) and none in *p*ABA or the glutamate tail. This combination of labeling was never observed. Similar logic ruled out misidentification of other folate species. In most cases, these deductions were confirmed based on species-specific fragmentation events (for example, $H_2PteGlu_n$ fragments between 2-amino-4-oxo-6-methylpterin and *p*ABA-Glu_n, whereas $H_4PteGlu_n$ fragments between H_4Pte and Glu_n).

Biochemical assays of FP-γ-GS activity. His-tagged version of the *E. coli folC* gene was expressed in *E. coli* strain BL21 under control of the *lacZ* promoter by induction with 1 mM IPTG. The resulting recombinant protein was purified on a Ni NTA agarose column (Qiagen). The peak-eluted fractions were used directly in enzyme assays. The reaction conditions were similar to those used previously for *in vitro* quantitation of FP-γ-GS activity[4,5]: 114 μg purified FP-γ-GS enzyme; 50 mM ammonium acetate buffer, pH 8.9; 5 mM ATP; 5 mM $MgCl_2$; 5 mM DTT; 5 mM glutamic acid; 100 μg ml^{-1} bovine serum albumin; and 100 μM $H_4PteGlu_1$ in a total volume of 100 μl and incubated at 37°C. Glutamate and ATP were assumed to be saturating in

all cases. The K_M of the enzyme for $H_4PteGlu_1$ was determined to be 50 μM (consistent with previous literature)[6] based on the $H_4PteGlu_1$ concentration-dependence of the extent of incorporation of [^{3}H]-glutamate into $H_4PteGlu_{2\text{-}3}$ over 30 min, as described by Shane[7]. The V_{max} of the enzyme preparation was measured to be 20 μM min^{-1} based on the rate of $H_4PteGlu_1$ consumption (and its conversion to $H_4PteGlu_2$ and $H_4PteGlu_3$) as determined by LC-MS/MS, with samples taken at various time points and fixed $H_4PteGlu_1$ concentration (100 μM).

The K_I for inhibition of FP-γ-GS by $H_2PteGlu_1$ was determined based on the extent of $H_4PteGlu_1$ consumption (measured by LC-MS/MS) as a function of $H_2PteGlu_1$ concentration added. The results were simulated assuming Michaelis-Menten kinetics with a single enzyme binding site for folates (i.e., $H_2PteGlu_1$ as a competitive inhibitor). The associated equations are as follows:

$$\frac{d[\mathrm{H_4PteGlu_1}]}{dt} = \frac{-V_{max}\cdot(\mathrm{H_4PteGlu_1})}{K_M\cdot\left(1+\frac{\mathrm{H_2PteGlu_1}}{K_I}+\frac{\mathrm{H_4PteGlu_1}}{K_M}+\frac{\mathrm{H_4PteGlu_2}}{K_M}\right)} \quad (5)$$

$$\frac{d[\mathrm{H_4PteGlu_2}]}{dt} = \frac{V_{max}\cdot(\mathrm{H_4PteGlu_1})}{K_M\cdot\left(1+\frac{\mathrm{H_2PteGlu_1}}{K_I}+\frac{\mathrm{H_4PteGlu_1}}{K_M}+\frac{\mathrm{H_4PteGlu_2}}{K_M}\right)} - \frac{V_{max}\cdot(\mathrm{H_4PteGlu_2})}{K_M\cdot\left(1+\frac{\mathrm{H_2PteGlu_1}}{K_I}+\frac{\mathrm{H_4PteGlu_1}}{K_M}+\frac{\mathrm{H_4PteGlu_2}}{K_M}\right)} \quad (6)$$

The simulation conditions were set to match the assay conditions: 100 μM $H_4PteGlu_1$ and varying concentrations of $H_2PteGlu_1$. K_I was determined to be 3.1 μM using a global optimizing method ("BFGS", also known as a variable metric algorithm, implemented in *R*) that minimized the sum of R^2 (where R is the difference between experimental and simulation concentrations) for $H_4PteGlu_1$.

Computer code for simulation of domino effect.

Script written in *R*.

```
# This file simulates the effect of the DHFR-inhibitor trimethoprim on folate
# metabolism.
#
# Authors:  Yun Kyung Kwon and Eugene Melamud, 2008

# Load libraries
library(odesolve) # library containing integrator
library(Hmisc)     # library containing functionality to plot error bars

######################## MODEL OF CONCENTRATION CHANGE ######################
# this function is called by integrator
# inputs:
#     x = concentrations
#     p = parameters
#     t = time
# output:
#     vector of dX/dt for DHF, DHF2, DHF3, THF, THF2, THF3

parms=c();
times=seq(0,125,0.1);  # show results for the following time points

# experimental initial (steady state) concentrations
ini=c(THF1=0.82, DHF1=0.022, THF2=2.15, DHF2=0.721, THF3=60.63, DHF3=39.65)

# comment out above line and use the line below to use simulated steady-state concentrations:
#ini=data[nrow(data), -1]

model <- function(t, x, p) {

# PARAMETERS

# Measured/calculated parameters:
  F1=2.8;  #In control cells, F1=2.8.  In trimethoprim-treated cells, F1=1.
  KI=3.1;
  Km=50;
  k1=0.05;
  k2=0.6;
  k3=1.2;
  k6=0.006;
  k4=2; # In control cells, k4=2.  In trimethoprim-treated cells, k4=0.03.

# Parameters manually selected to mimic experimental behaviors:
  k5=0.03;
  Vmax=60;
```

```
# DERIVATIVES

  dx1=x[2]*k4-x[1]*k1-((Vmax*x[1]/Km)/(1+x[2]/KI+x[4]/KI+x[1]/Km+x[3]/Km));
  dx2=F1+x[1]*k1-x[2]*k4-x[2]*k5;
  dx3=x[4]*k4-x[3]*k2+(Vmax*x[1]/Km)/(1+x[2]/KI+x[4]/KI+x[1]/Km+x[3]/Km)-
        (Vmax*x[3]/Km)/(1+x[2]/KI+x[4]/KI+x[1]/Km+x[3]/Km);
  dx4=x[3]*k2-x[4]*k4-x[4]*k5;
  dx5=x[6]*k4-x[5]*k3+(Vmax*x[3]/Km)/(1+x[2]/KI+x[4]/KI+x[1]/Km+x[3]/Km)-x[5]*k6;
  dx6=x[5]*k3-x[6]*k4-x[6]*k5;

  THF1=x[1];
  DHF1=x[2];
  THF2=x[3];
  DHF2=x[4];
  THF3=x[5];
  DHF3=x[6];

# RETURN LIST OF DERIVATIVES
  list(c(dx1,dx2,dx3,dx4,dx5,dx6))
}

data=lsoda(ini,times,model,parms,rtol=1e-4, atol= 1e-5)

########################## EXPERIMENTAL CONCENRATIONS ########################

# x-axis: time points
x = c(0, 6, 10, 20, 35, 65, 125)

# experimental DHF concentrations
oDHF1 = c(0.022, 2.05, 2.61, 3.86, 6.15, 7.49, 7.16);
# experimental DHF standard error
DS1 = c(0.002, 0.37, 0.58, 0.02, 1.08, 0.19, 2.65);

# experimental reduced monoglutamte folate species concentrations
# (sum of MTHF, THF, and methylene-THF)
oMTHF1 = c(0.87, 0.48, 0.74, 1.88, 1.53, 3.64, 3.27);
# experimental reduced monoglutamte folate species standard error
MS1 = c(0.30, 0.02, 0.23, 0.61, 0.30, 0.51, 0.74);

# experimental DHF2 concentrations
oDHF2 = c(0.721, 5.11, 4.56, 5.58, 6.11, 11.36, 16.42);
# experimental DHF2 standard error
DS2 = c(0.57, 1.23, 1.13, 0.63, 1.11, 0.60, 3.42);

# experimental reduced diglutamte folate species concentrations
# (sum of MTHF2, THF2, and methylene-THF2)
oMTHF2 = c(2.33, 3.32, 2.02, 1.31, 3.92, 8.65, 10.93);
# experimental reduced diglutamte folate species standard error
MS2 = c(0.23, 0.32, 0.16, 0.09, 0.54, 1.08, 1.00);
```

```
# experimental DHF3 concentrations
oDHF3 = c(39.65, 130.69, 86.94, 108.88, 69.11, 33.28, 14.35);
# experimental DHF3 standard error
DS3 = c(10.38, 19.17, 49.37, 57.02, 19.95, 0.84, 0.69);

# experimental reduced triglutamte folate species concentrations
# (sum of MTHF3, THF3, and methylene-THF3)
oMTHF3 = c(93.56, 15.57, 9.34, 6.10, 3.11, 2.38, 1.13);
# experimental reduced triglutamte folate species standard error
MS3 = c(22.99, 4.18, 2.24, 1.66, 0.87, 1.09, 0.45);

##################################### PLOTS #####################################
# plot experimental and simulated concentrations

   par(mfrow=c(2,3),cex.lab=1.4,cex.axis=.94,las=1);

   plot(data[,'time'],data[,'DHF1'],log="y",yaxt="n",type="l",col=3,lwd=3,
   xlab='Time (min)',ylab=expression(mu*M),ylim=c(0.01,200),bty='l');
   title(main=expression(H[2]*PteGlu[1]),cex.main=1.8);
   axis(2,c(0.01,0.1,1,10,100),labels=c(0.01,0.1,1,10,100));
   points(x,oDHF1,pch=15,cex=2,bty='l',col=1);
   errbar(x,oDHF1,oDHF1+DS1,oDHF1-DS1,add=TRUE,col=1);

   plot(data[,'time'],data[,'DHF2'],log="y",yaxt="n",type="l",col=3,lwd=3,
   xlab='Time (min)',ylab=expression(mu*M),ylim=c(0.01,200),bty='l');
   title(main=expression(H[2]*PteGlu[2]),cex.main=1.8);
   axis(2,c(0.01,0.1,1,10,100),labels=c(0.01,0.1,1,10,100));
   points(x,oDHF2,pch=15,cex=2,bty='l',col=1);
   errbar(x,oDHF2,oDHF2+DS2,oDHF2-DS2,add=TRUE,col=1);

   plot(data[,'time'],data[,'DHF3'],log="y",yaxt="n",type="l",col=3,lwd=3,
   xlab='Time (min)',ylab=expression(mu*M),ylim=c(0.01,200),bty='l');
   title(main=expression(H[2]*PteGlu[3]),cex.main=1.8);
   axis(2,c(0.01,0.1,1,10,100),labels=c(0.01,0.1,1,10,100));
   points(x,oDHF3,pch=15,cex=2,bty='l',col=1);
   errbar(x,oDHF3,oDHF3+DS3,oDHF3-DS3,add=TRUE,col=1);

   plot(data[,'time'],data[,'THF1'],log="y",yaxt="n",type="l",col=4,lwd=3,
   xlab='Time (min)',ylab=expression(mu*M),ylim=c(0.01,200),bty='l');
   title(main=expression(H[4]*PteGlu[1]),cex.main=1.8);
   axis(2,c(0.01,0.1,1,10,100),labels=c(0.01,0.1,1,10,100));
   points(x,oMTHF1,pch=15,cex=2,bty='l',col=1);
   errbar(x,oMTHF1,oMTHF1+MS1,oMTHF1-MS1,add=TRUE,col=1);

   plot(data[,'time'],data[,'THF2'],log="y",yaxt="n",type="l",col=4,lwd=3,
   xlab='Time (min)',ylab=expression(mu*M),ylim=c(0.01,200),bty='l');
   title(main=expression(H[4]*PteGlu[2]),cex.main=1.8);
   axis(2,c(0.01,0.1,1,10,100),labels=c(0.01,0.1,1,10,100));
```

```
points(x,oMTHF2,pch=15,cex=2,bty='l',col=1);
errbar(x,oMTHF2,oMTHF2+MS2,oMTHF2-MS2,add=TRUE,col=1);

plot(data[,'time'],data[,'THF3'],log="y",yaxt="n",type="l",col=4,lwd=3,
xlab='Time (min)',ylab=expression(mu*M),ylim=c(0.01,200),bty='l');
title(main=expression(H[4]*PteGlu[3]),cex.main=1.8);
axis(2,c(0.01,0.1,1,10,100),labels=c(0.01,0.1,1,10,100));
points(x,oMTHF3,pch=15,cex=2,bty='l',col=1);
errbar(x,oMTHF3,oMTHF3+MS3,oMTHF3-MS3,add=TRUE,col=1);
```

SUPPLEMENTARY REFERENCES

1. Yuan, J., Fowler, W.U., Kimball, E., Lu, W. & Rabinowitz, J.D. Kinetic flux profiling of nitrogen assimilation in *Escherichia coli*. *Nat Chem Biol* **2**, 529-530 (2006).
2. Gutnick, D., Calvo, J.M., Klopotowski, T. & Ames, B.N. Compounds Which Serve as the Sole Source of Carbon or Nitrogen for *Salmonella typhimurium* LT-2. *J. Bacteriol.* **100**, 215-219 (1969).
3. Brauer, M.J. et al. Conservation of the metabolomic response to starvation across two divergent microbes. *Proceedings of the National Academy of Sciences* **103**, 19302-19307 (2006).
4. Masurekar, M. & Brown, G.M. Partial purification and properties of an enzyme from *Escherichia coli* that catalyzes the conversion of glutamic acid and 10-formyltetrahydropteroylglutamic acid to 10-formyltetrahydropteroyl-gamma-glutamylglutamic acid. *Biochemistry* **14**, 2424-2430 (1975).
5. Ferone, R. & Warskow, A. Co-purification of dihydrofolate synthetase and N10-formyltetrahydropteroyldiglutamate synthetase from *E. coli*. *Adv Exp Med Biol* **163**, 167-81 (1983).
6. Sheng, Y. et al. Mutagenesis of Folylpolyglutamate Synthetase Indicates That Dihydropteroate and Tetrahydrofolate Bind to the Same Site. *Biochemistry* **47**, 2388-2396 (2008).
7. Shane, B. Pteroylpoly(gamma-glutamate) synthesis by Corynebacterium species. Purification and properties of folypoly(gamma-glutamate) synthetase. *J. Biol. Chem.* **255**, 5655-5662 (1980).